Global Research journal of Natural Science and Technology (Grjnst)
Volume: 03 - Issue 4 (2025)
p.ISSN: 2790-7643 e.ISSN: 2790-7651
www.grjnst.com

# A Synergistic Ag-Fe/rGO Photocatalyst for the Visible-Light Degradation and Detoxification of 2-Nitrophenol

**Imtiaz Hussain**
*Faculty of Sciences, Superior University Lahore, Lahore 54000, Pakistan*
**Ayesha Kanwal**
*Institute of Chemistry, University of Sargodha, Sargodha 40100, Pakistan*
**Muhammad Ashraf Shaheen (Corresponding Author)**
*Faculty of Sciences, Superior University Lahore, Lahore 54000, Pakistan*
*Email: masaheen1964@gmail.com*

**Muhammad Azhar Abbas**
*Institute of Chemistry, University of Sargodha, Sargodha 40100, Pakistan/ Government Ambala Muslim Graduate College, Sargodha 40100, Pakistan*

## Abstract

Ag-Fe engineered on Reduced graphene oxide (Ag-Fe/rGO) was prepared and analysed as an effective photocatalyst in the degradation of 2-Nitrophenol (2-NP) suspended in water. The catalyst was also highly active as it was able to degrade almost fully when exposed to visible light in a minimal reaction time. The kinetic study revealed that the degradation was of pseudo-first-order and the rate constants grew with increase in temperature. The thermodynamic researches indicated the activation energy of about 50.0 kJ $mol^{-1}$ and also indicated that there is a kinetically controlled reaction whereas the positive change in entropy indicated an increase in disorder in the formation of the activated complex. The Ag-Fe/rGO photocatalyst was highly stable and reusable during a series of cycles, and the activity decreased only slightly. The mechanistic studies revealed that synergistic effects of Ag-Fe nanoparticles (Ag-Fe NPs) and the rGO contribute to the favorable charge separation and the increase in reactive oxygen species (OH and $O^{2-}$), which dominated the oxidative degradation of 2-NP. The results show that Ag-Fe/rGO is a potential, reusable, and very effective photocatalyst in the decontamination of nitroaromatic pollutants in water, and can be used in practical applications in the treatment of waste water.

**Keywords:** Ag-Fe NPs, reduced graphene oxide, 2-nitrophenol, photocatalytic degradation, pseudo-first-order kinetics, reactive oxygen species, catalyst reusability, activation energy

## 1. Introduction

The high rate of industrialization and urbanization has contributed to the constant release of organic wastes that are harmful to the environment and to the human health [1]. Nitroaromatic compounds are the worst of these pollutants since they are highly toxic, stable chemically, and not readily treated using traditional biological processes. These are commonly found in the industrial effluents because they are commonly utilized in industries including pharmaceuticals, dyes, petrochemicals, pesticides and explosives [2]. The inability to eliminate nitroaromatic contaminants in the aquatic system may lead to a long-term ecological and devastating health impacts, which are mutagenic and carcinogenic even at low levels [3].

An example of a nitroaromatic compound which has attracted much focus is 2-nitrophenol (2-NP) which is highly soluble in water and toxic in nature. It is mostly observed in the wastewater streams of dye manufacturing, resin production and the agrochemicals industries [4]. 2-NP is highly recalcitrant to natural degradation, because of its stable aromatic structure and electron-withdrawing nitro group and therefore, it would be difficult to remove this compound in wastewater [5]. The traditional ways of treatment including adsorption has been successfully applied by modifying the natural polysaccharides because of the non-toxic, stimuli-sensitive, and chemically modifiable nature of them [6-26]. The design of effective low cost and environmental friendly methods to degrade 2-NP is therefore a high research agenda.

Metal-based nanomaterials as catalysts in reducing nitrophenolic compounds under mild conditions of reaction have become an effective method to degrade these compounds. The method has a fast reaction kinetics, and high conversion level, and low levels of production of toxic byproducts [27]. Specifically, it has been shown that noble metal nanoparticles (NPs) like silver (Ag) have an optimal catalysis activity because of their large surface energy and electric transfer potential [28]. Beyond noble metals, semiconductor nanomaterials such as NiO, CdO, ZnO, and sulfur quantum dots have been widely employed for dye degradation and antibacterial applications [29-32]. The practical use of monometallic Ag catalysts is, however, hampered by the challenges posed by aggregation, low durability, and high cost of the material [33]. Such constraints have prompted increased attention towards the design of bimetallic catalysts, in which a noble metal is coupled with a transition metal, which can be shown that catalytic performance can be greatly improved through the combined effects [34].

Iron (Fe) has received a lot of interest as a second best metal because of its low cost, environmental friendliness and redox property. To enhance the electron mobility, active site availability, and facilitate interfacial charge transfer during catalytic reactions the addition of Fe to Ag-based catalytic systems can be done [35]. In addition, the Fe-based catalysts can have magnetic properties, which can readily be separated and reutilized, making them more applicable in the treatment of wastewater in practice [36]. The synergetic effect between Ag

and Fe is therefore capable of giving rise to increased catalytic activity with a decrease in the total noble metal content [37].

The selection of a proper support material is also very important to high catalytic performance [38-40]. The graphene oxide (GO) has become an outstanding support, since it has a large specific surface area, excellent electrical conductivity, mechanical stability, and the affinity with metal nanoparticles [41]. The two-dimensional geometry of Reduced Graphene Oxide (rGO) offers a large number of anchoring sites, which is a practical solution to the problem of NPs agglomeration and provides efficient dispersion of active metal species [42]. Moreover, rGO ensures quick electron-carrying during catalytic reactions and this is of essence especially through reduction reactions of nitroaromatic compounds.

The Ag-Fe NPs engineering onto rGO will be a combination of bimetallic synergy and carbon-based support material, thus creating a multifunctional catalytic system [43]. The catalyst stability and electron transfer are increased with the presence of rGO, and the catalytic activity and recyclability are increased with the Ag-Fe interaction [44]. These integrated nanocomposites have been found to have high potential in environmental clean up processes especially in the degradation of toxic organic products in aqueous environments [45, 46].

This paper has reported the development and testing of an Ag-Fe modified GO composite as a catalyst that degrades 2-NP in water. A model reduction system was used to investigate the degradation performance under ambient conditions and also the reusability of the catalyst was tested. The findings reveal the potential of the Ag-Fe/rGO material as an effective, green and reusable catalyst in the treatment of nitrophenol-contaminated water waste, and as a part of the green and viable water purification technologies.

## 2. Materials and Method

### 2.1. Materials

The synthesis of GO was done by using graphite powder. The precursors of Ag and Fe used in the formation of the bimetallic catalyst were silver nitrate ($AgNO_3$) and Fe salt. In order to carry out catalytic degradation tests, sodium borohydride ($NaBH_4$) was chosen as the reducing agent and 2-NP as the model organic pollutant to degrade. Analytical grade chemicals were used without purification. All the experimental procedures were done using deionized water.

### 2.2. Method

#### 2.2.1. Preparation of rGO

The modified oxidation technique was used to prepare graphene oxide using the graphite powder. The resulting graphene oxide was dispersed in deionized water then reduced under regulated conditions to get reduced graphene oxide. The final rGO was well washed in deionized water to eliminate remaining impurities and dried to be used.

### 2.2.2. Synthesis of Ag-Fe/rGO Composite

The Ag-Fe composite of GO engineered was produced using a wet chemical reduction method. The rGO was dispersed in deionized water at first using an ultrasound to obtain a homogenous suspension. Calculated volumes of Ag and Fe precursor solutions were added into the suspension with constant stirring. A reducing agent was also incorporated slowly to enable reduction of the metal ions and deposition to be done on the rGO surface concurrently. A certain period of time was given to the reaction mixture to ensure that Ag and Fe species are incorporated effectively. The resultant composite was separated through magnetic separation or centrifugation, washed many times using deionized water and dried at moderate temperature.

### 2.3. Catalytic Degradation of 2-NP

Reduction of 2-NP in aqueous solution at room temperature was used to determine the catalytic activity of the Ag- Fe/rGO composite. In a standard experiment, 2-NP solution of known concentration was added to freshly prepared $NaBH_4$ in the presence of a stirring program. After a certain amount of Ag-Fe/rGO catalyst was added, the reaction was then started and followed at regular time intervals. The degradation was measured by monitoring the reduction in individual absorbance of 2-NP through the use of UV- visible spectroscopy.

### 2.4. Reusability Studies

The Ag-Fe/rGO composite was recovered following every reaction cycle through the use of magnetic separation in order to determine the stability and recyclability of the catalyst. The catalyst was recovered and washed with deionized water and dried and reused again in subsequent degradation run with the same conditions [47].

## 3. Results and Discussion

### 3.1. Degradation of 2-NP

UV-Vis spectroscopy was used to monitor the degradation of 2-NP over Ag-Fe/rGO as shown in Fig. 1(A). The typical absorption maximum of 2-NP at the wavelength of around 400 nm kept on decreasing with reaction time, which demonstrated effective catalytic degradation [48, 49]. There are no new prominent peaks, which implies that the process is carried out through oxidative degradation and not by simple adsorption. The synergistic effect of Ag-Fe NPs and rGO contributes to the high catalytic activity through the following: high surface area, high electron transport, and multiple active sites. The conductive rGO framework can not only allow the movement of electrons but also inhibit recombination of charges that suppresses the creation of reactive oxygen species (ROS) essential in degrading pollutants. Ag-Fe/rGO shows a high rate of degradation as compared to that of bare Ag or Fe NPs, which supports the significance of nanoparticle engineering and graphene-based supports.

#### 3.1.1. Kinetics of Degradation

The degradation kinetics were analyzed using the pseudo-first-order model:

$$\ln \frac{A_o}{A_f} = kt \qquad \text{Eq. (1)}$$

Where $A_0$ and A are the absorbance of 2-NP at initial and time "t" respectively, and "k" is the rate constant. Linear plots of $\ln(A_0/A)$ versus time as represented in Fig. 1(b), at different temperatures yielded high correlation coefficients ($R^2 = 0.987–0.994$), confirming pseudo-first-order behavior. The temperature of the reaction raised the slope of the line, which is an indication of higher reaction rates. Such tendency implies the increase in temperature stimulates molecular collisions and surface adsorption of 2-NP on Ag-Fe/rGO active sites. The measured rate constants were also greater than those of other graphene-supported catalysts which highlights the high performance of the designed Ag-Fe NPs. Also, the pseudo-first-order behavior confirms that the degradation is catalyzed mainly by the surface and the concentration of the catalyst is kept constant and the rate of the reaction is influenced by the concentration of the pollutant (31).

### 3.1.2. Degradation Efficiency at Different Temperatures

The percentage degradation of 2-NP was calculated as:

$$Degradation(\%) = \frac{A_0 - A}{A_0} \times 100 \qquad \text{Eq. (2)}$$

The findings indicated that there was an obvious rise in the efficiency of degradation with reaction time and temperature as depicted in Fig. 1(c). Nevertheless, at 328 K, a near-complete degradation was obtained in 50 minutes whereas the process was slower at 298 K. This temperature response suggests a higher kinetic energy, a greater transfer of mass and quicker reactions of redox at higher temperatures. This trend also shows that the catalytic activity of Ag-Fe/rGO is thermally-assisted, and the rGO support increases the movement of electrons, and, therefore, enables a generation of reactive species to be efficient. The data indicate that thermal energy can be used to overcome the activation barriers and allow pollutant adsorption and further degradation of pollutants on the catalyst surface (32).

### 3.1.3. Thermodynamic Parameters

The temperature effect on reaction rate constants follows the Arrhenius equation:

$$k = Ae^{-E_a/RT}$$

$$\ln k = \ln A - \frac{E_a}{RT} \qquad \text{Eqs. (3, 4)}$$

Where "$k$" is the rate constant, "$A$" is the pre-exponential factor, "$E_a$" is activation energy, "$R$" is the gas constant, and "$T$" is absolute temperature. The calculated $E_a \approx 50.0$ kJ mol$^{-1}$) shown in Fig. 1(d) indicates a kinetically controlled process.

Additional thermodynamic parameters were calculated using the Eyring equation:

$$\ln(\frac{k}{T}) = -\frac{\Delta H}{RT} + \frac{\Delta S}{R} + \ln(\frac{k_B}{h}) \qquad \text{Eq. (5)}$$

and the Gibbs free energy of activation:

$$\Delta G = \Delta H - T\Delta S \qquad \text{Eq. (6)}$$

Positive $\Delta H$ and $\Delta G$ suggest the process is endothermic and non-spontaneous at lower temperatures, while positive $\Delta S$ indicates increased disorder during formation of the activated complex on the Ag–Fe/rGO surface.

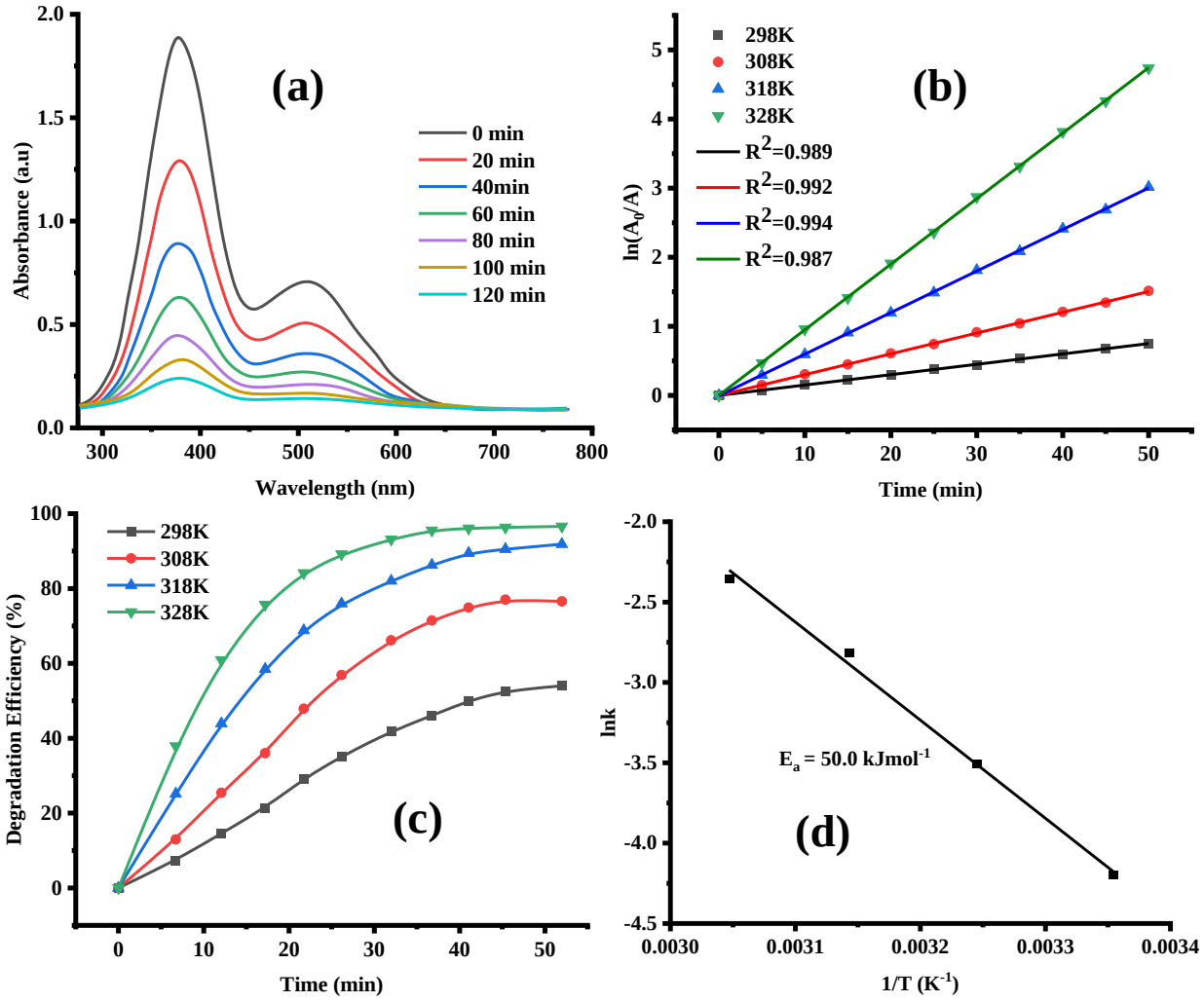

**Fig. 1.** (A) UV-Vis adsorption spectra of 2-NP solution at different radiation exposure time in the presence of catalyst Ag-Fe/rGO (B) Plot of % dye degradation efficiency versus time (C) Pseudo-first-order kinetics model fitting of experimental degradation data of 2-NP at different temperatures (D) Plot of lnk versus 1/T.

### 3.1.4. Photocatalyst Regeneration and Reusability

Ag-Fe/rGO stability was tested in five cyclic degradation cycles as represented in Fig. 2(a). The catalyst was very degradation efficient and there was minimal loss of catalyst efficiency after repeated usage. Surface fouling or leaching of NPs partially can be considered a minor loss of activity. The findings validates the integrity of structure and viability of Ag-Fe/rGO in terms of reusability. This stability is important to the actual wastewater treatment, because it saves the cost of the operation and also pollutant removal is always guaranteed (33). The comparison with other graphene-based metal catalysts indicate that the designed Ag-Fe combination offers better durability and is active over several cycles with so-called active sites.

### 3.1.5. Proposed Mechanism

A plausible mechanism for 2-NP degradation over Ag–Fe/rGO involves the generation of reactive oxygen species (ROS) and stepwise oxidative reactions:

**Step 1. Photoexcitation of Ag–Fe NPs:**

$$\bullet OH / \bullet O_2^- + 2-NP \rightarrow \text{int}ermediates \rightarrow CO_2 + H_2O \quad Ag-Fe/rGO + h\nu \rightarrow e^- + h^+$$

**Step 2. Electron transfer to rGO:**

$$e^-_{Ag-Fe} \rightarrow e^-_{rGO}$$

The rGO support acts as an electron sink, suppressing charge recombination.

**Step 3. Formation of reactive oxygen species**

$$e^- + O_2 \rightarrow \bullet O_2^-, \quad h^+ + H_2O \rightarrow \bullet OH + H^+$$

**Step 4. Oxidative degradation of 2-NP**

$$\bullet OH / \bullet O_2^- + 2-NP \rightarrow \text{int}ermediates \rightarrow CO_2 + H_2O$$

The synergistic effect of Ag-Fe NPs and rGO allows the effective separation of charges and the production of ROS. Nitroaromatic ring is attacked by hydroxyl and superoxide radicals and the mineralization happens in stages. The experiments on scavengers showed that degradation efficiency is significantly reduced under the condition of radical quenchers, meaning that

reactive oxygen species are important factors in the photocatalytic degradation of 2-nitrophenol over Ag-Fe/rGO as shown in Fig. 2(b). The process is the reason why the mechanism is highly degraded and temperature dependent in kinetic studies.

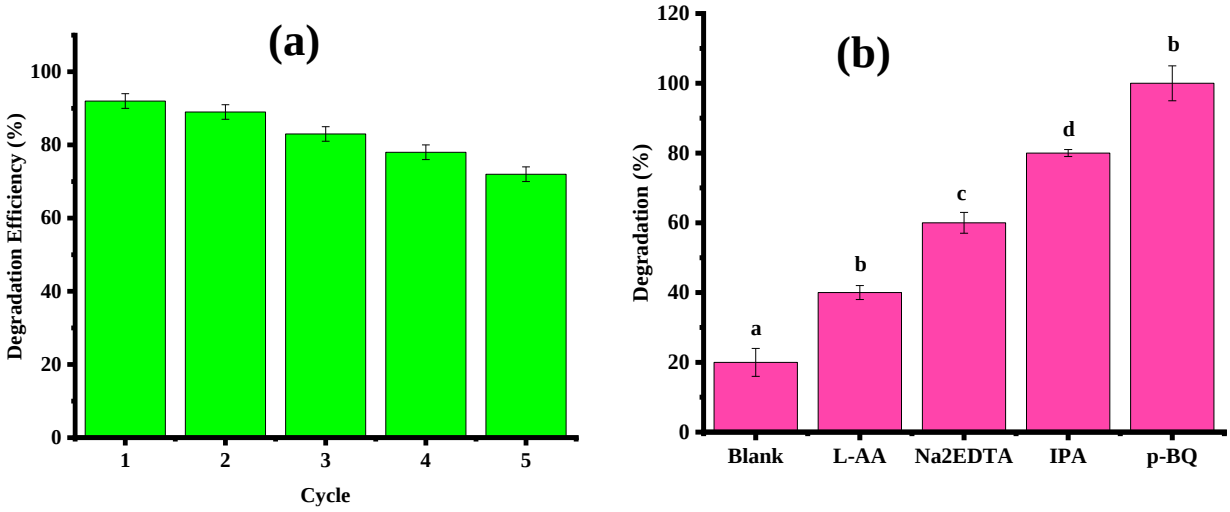


**Fig. 2.** (B) Photocatalyst regenerataion, plot of degradation efficiency (%) versus cycles (C) Degradation efficiency of different radicals. Different letters denote significantly different ($P < 0.05$) results compared among cycles and radical scavengers.

## 4. Conclusion

This paper has managed to synthesize Ag-Fe engineered Reduced graphene oxide (Ag-Fe/rGO) that was utilized as an effective photocatalyst in the degradation of 2-Nitropenol (2-NP). The catalyst was very active as it degraded quickly (in a few seconds) and almost completely when irradiated by visible light. Kinetic studies showed that the degradation was pseudo first-order, and rate constants were higher at higher temperature. Thermodynamic results revealed the presence of an activation energy of about 50.0 kJ mol-1 which confirmed that the process was kinetically controlled and endothermic as well as the positive change in entropy indicated that more disorder was generated during the formation of the activated complex. Ag-Fe/rGO catalyst was also characterized by high stability and reusability after several cycles and thus makes it applicable in practice. The hypothesized mechanism showed that synergistic effects of Ag-Fe NPs with rGO increased charge separation and reactive oxygen species subsequent to which was found to be the most obvious contributor to the oxidative disintegration of 2-NP. As a whole, this literature shows that Ag-Fe/rGO is potentially a good, reusable, and efficient photocatalyst in lauding the removal of nitroaromatic pollutants in aqueous environments.

## Reference

[1] Sharma, B., Vaish, B., Monika, Singh, U.K., Singh, P. and Singh, R.P., 2019. Recycling of organic wastes in agriculture: an environmental perspective. International journal of environmental research, 13(2), 409-429.

[2] Tiwari, J., Tarale, P., Sivanesan, S. and Bafana, A., 2019. Environmental persistence, hazard, and mitigation challenges of nitroaromatic compounds. Environmental science and pollution research, 26(28), 28650-28667.

[3] Kumari, S., Kumari, S., Sankhla, M.S., Gautam, A., Sharma, T., Sharma, A., Awasthi, G. and Awasthi, K.K., 2023, December. Xenobiotics-Induced Water Contamination and Adverse Effects on Aquatic Organism. In International Conference on "Recent Trends in Environment and Sustainable Development (pp. 1409-1428). Cham: Springer Nature Switzerland.

[4] Haleem, A., Shafiq, A., Chen, S.Q. and Nazar, M., 2023. A comprehensive review on adsorption, photocatalytic and chemical degradation of dyes and nitro-compounds over different kinds of porous and composite materials. Molecules, 28(3), 1081.

[5] Rashid, R., Shafiq, I., Akhter, P., Iqbal, M.J. and Hussain, M., 2021. A state-of-the-art review on wastewater treatment techniques: the effectiveness of adsorption method. Environmental Science and Pollution Research, 28(8), pp.9050-9066.

[6] Ali, A., Akram, A., Bakar, M.A., Amin, H.M., Zohra, L., Abbas, A., Sher, M., Hussain, M.A., Haseeb, M.T. and Imran, M., 2025. A model batch and column study for Cd (II) uptake using citric acid cross-linked *Salvia spinosa* hydrogel: Optimization through Box-Behnken design. Journal of Industrial and Engineering Chemistry, 151, 746-761.

[7] Hussain, A., Fatima, S., Abbas, A., Ali, A., Amin, M., Muhammad, G. and Sher, M., 2023. Removal of Cr (III) and Ni (II) from aqueous solution using a mixed cellulose ether-ester hydroxyethylcellulose adipate. Desalination and Water Treatment, 283, 153-163.

[8] Hussain, M.A., Gul, S., Abbas, A., Ali, A. and Alotaibi, N.F., 2021. Chemically modified rhamnogalacturonans from linseed: a supersorbent for $Cd^{2+}$ and $Pb^{2+}$ uptake from aqueous solution. Desalination and Water Treatment, 221, 163-175.

[9] Shehzad, M.K., Ali, A., Qasim, S., Mumtaz, A., Hussain, M.A., Fawy, K.F., Nishan, U., Azhar, I., Abbas, M.A. and Abba, A., 2025. Sustainable remediation of cadmium using succinate-functionalized glucoxylan from chia (*Salvia hispanica*) seeds hydrogel. Journal of Industrial and Engineering Chemistry. https://doi.org/10.1016/j.jiec.2025.10.034

[10] Ali, A., Haseeb, M.T., Hussain, M.A., Tulain, U.R., Muhammad, G., Azhar, I., Hussain, S.Z., Hussain, I. and Ahmad, N., 2023. A pH responsive and superporous biocomposite hydrogel of *Salvia spinosa* polysaccharide-co-methacrylic acid for intelligent drug delivery. RSC Advances, 13(8), 4932-4948.

[11] Ali, A., Hussain, M.A., Haseeb, M.T., Farid-Ul-Haq, M., Erum, A. and Hussain, M., 2024.

Acute toxicity studies of methacrylic acid based composite hydrogel of *Salvia spinosa* seed mucilage: a potential non-toxic candidate for drug delivery. Cellulose Chemistry and Technology, 58(1-2), 45-53.

[12] Ali, A., Hussain, M.A., Haseeb, M.T., Tulain, U.R., Farid-ul-Haq, M., Tabassum, T., Muhammad, G., Hussain, S.Z., Hussain, I. and Erum, A., 2023. Synthesis, characterization, and acute toxicity of pH-responsive *Salvia spinosa* mucilage-co-acrylic acid hydrogel: A smart excipient for drug release applications. Reactive and Functional Polymers, 182, 105466.

[13] Ali, A., Hussain, M.A., Abbas, A., Khan, T.A., Muhammad, G., Haseeb, M.T. and Azhar, I., 2022. Comparative isoconversional thermal analysis and degradation kinetics of *Salvia spinosa* (Kanocha) seed hydrogel and its acetates: a potential matrix for sustained drug release. Cellulose Chemistry Technolog, 56(3-4), 239-250.

[14] Ali, A., Hussain, M.A., Haseeb, M.T., Ashraf, M.U., Farid-ul-Haq, M., Tabassum, T., Muhammad, G. and Abbas, A., 2023. pH-responsive, hemocompatible, and non-toxic polysaccharide-based hydrogel from seeds of *Salvia spinosa* L. for sustained release of febuxostat. Journal of the Brazilian Chemical Society, 34, 906-917.

[15] Rehman, A.U., Maqsood, A., Siddique, A.B., Akhtar, S., Fawy, K.F., Ain, Q.U., Sher, M., Nishan, U., Ahmad, T., Ali, A. and Abbas, A., 2025. From waste to water treatment: Banana peel powder for polystyrene removal with FTIR-based mechanistic understanding. Journal of Industrial and Engineering Chemistry. https://doi.org/10.1016/j.jiec.2025.11.036

[16] Ali, A., Hussain, M.A., Haseeb, M.T., Bukhari, S.N.A., Tabassum, T., Farid-ul-Haq, M. and Sheikh, F.A., 2022a. A pH-responsive, biocompatible, and non-toxic citric acid cross-linked polysaccharide-based hydrogel from *Salvia spinosa* L. offering zero-order drug release. Journal of Drug Delivery Science and Technology, 69, 103144.

[17] Amjad, F., Ali, A., Hussain, M.A., Haseeb, M.T., Ajaz, I., Farid-ul-Haq, M., Hussain, S. Z. and Hussain, I., 2025. A superabsorbent and pH-responsive copolymer-hydrogel based on glucomannans from *Ocimum basilicum* (sweet basil): A smart and non-toxic material for intelligent drug delivery. International Journal of Biological Macromolecules, 315(2), 144452.

[18] Ali, A., Haseeb, M.T., Hussain, M.A., Muhammad, T., Muhammad, G., Ahmad, N., Alotaibi, N.F., Hussain, S.Z. and Hussain, I., 2022. Extraction optimization of a superporous polysaccharide-based mucilage from *Salvia spinosa* L. Cellulose Chemistry and Technology, 56, 957-969.

[19] Iqbal, J., Kanwal, M., Siddique, A., Fawy, K.F., Sher, M., Nishan, U., ur Rehman, M.F., Abbas, M.A., Ali, A. and Abbas, A., 2025. β-Cyclodextrin-functionalized silver nanoparticles as a visual probe for selective tetrahydrocannabinol detection via host–guest induced plasmonic shifts. Microchemical Journal, 116177.

[20] Hussain, M.A., Shahzad, K., Ali, A., Haseeb, M.T. and Hussain, S.Z., 2025. Development

of a novel smart bio-composite hydrogel based on dextran, citric acid, and glucoxylan for pH-dependent drug delivery and stimuli-responsive swelling and release. Polymers and Polymer Composites, 33, p.09673911251350240.

[21] Khatoon, M., Ali, A., Hussain, M.A., Haseeb, M.T., Muhammad, G., Sher, M., Hussain, S.Z., Hussain, I. and Iqbal, M., 2025. A chia (*Salvia hispanica* L.) seed mucilage-based glucoxylan-grafted-acrylic acid hydrogel: a smart material for pH-responsive drug delivery systems. Materials Advances, 6(8), 2636-2647.

[22] Hussain, M.A., Raees, N., Ali, A., Tayyab, M., Muhammd, G., Uroos, M. and Batool, M., 2025. Optimization of rhamnogalacturonan extraction from linseed using RSM and designing a pH-responsive tablet formulation for sustained release of ciprofloxacin. Cellulose Chemistry and Technology, 59, 547-558.

[23] Hussain, M.A., Taj, T., Ali, A., Haseeb, M.T., Hussain, S.Z., Muhammad, G. and Bukhari, S.N.A., 2025. Cross-Linking of Hydroxypropylcellulose With Flaxseed Rhamnogalacturonans Using Citric Acid Produces a Hemocompatible Biocomposite for pH-Responsive Rifaximin Delivery. Journal of Applied Polymer Science, e57486.

[24] Hussain, M.A., Abbas, A., Yameen, E., Ali, A., Muhammad, G., Hussain, M. and Shafiq, Z., 2022. Adsorptive removal of $Pb^{2+}$ and $Cu^{2+}$ from aqueous solution using an acid modified glucuronoxylan-based adsorbent. Desalination and Water Treatment, 248, 163-175.

[25] Hussain, M.A., Abbas, A., Habib, M.G., Ali, A., Farid-ul-Haq, M., Hussain, M., Shafiq, Z. and Irfan, M.I., 2021. Adsorptive removal of Ni (II) and Co (II) from aqueous solution using succinate-bonded polysaccharide isolated from Artemisia vulgaris seed mucilage. Desalination and Water Treatment, 231, 182-195.

[26] Ali, A., Hussain, M.A., Abbas, A., Haseeb, M.T., Azhar, I., Muhammad, G., Hussain, S.Z., Hussain, I. and Alotaibi, N.F., 2023. Succinylated *Salvia spinosa* hydrogel: Modification, characterization, cadmium-uptake from spiked high-hardness groundwater and statistical analysis of sorption data. Journal of Molecular Liquids, 376, 121438.

[27] Das, T.K. and Das, N.C., 2022. Advances on catalytic reduction of 4-nitrophenol by nanostructured materials as benchmark reaction. International Nano Letters, 12(3), 223-242.

[28] Zada, A., Muhammad, P., Ahmad, W., Hussain, Z., Ali, S., Khan, M., Khan, Q. and Maqbool, M., 2020. Surface plasmonic-assisted photocatalysis and optoelectronic devices with noble metal nanocrystals: design, synthesis, and applications. Advanced Functional Materials, 30(7), 1906744.

[29] Siddique, A.B., Shaheen, M.A., Shafeeq, S., Abbas, A., Zaman, Y., Ishaque, M.Z. and Aslam, M., 2025. Optimization of photodegradation of crystal violet dye and biomedical applications of greenly synthesized NiO nanoparticles. Materials Advances, 6(4), 1330-1344.

[30] Shen, L., Chen, X., Chen, Y., Peng, J., Abbas, A., Wei, J., Yu, C., Li, J. and Li, Y., 2022. One-Step Hydrothermal Synthesis of Sulfur Quantum Dots for Photoelectrochemical Catalysis for Dye Degradation. Journal of Electronic Materials, 51(6).

[32] Ahmad, H., Siddique, A.B., Zaheer, S., Sattar, R., Abbas, A., Amin, M., Al-Salahi, R., Abuelizz, H.A. and Saleem, M.Z., 2025. Energy bandgap tuning of Sr-doped ZnO nanoparticles for photodegradation of azo dyes and antibacterial applications. Journal of Water Process Engineering, 74, 107855.

[32] Siddique, A.B., Shaheen, M.A., Abbas, A., Zaman, Y., Ishaque, M.Z., Shami, A., Aslam, M., Alsyaad, K.M. and Ali, A., 2025. Highly efficient greenly synthesized cadmium oxide nanoparticles for methyl orange degradation, antibacterial and antioxidant applications. Journal of Molecular Structure, 1331, 141566.

[33] Sharma, R.K., Yadav, S., Dutta, S., Kale, H.B., Warkad, I.R., Zbořil, R., Varma, R.S. and Gawande, M.B., 2021. Silver nanomaterials: synthesis and (electro/photo) catalytic applications. Chemical Society Reviews, 50(20), 11293-11380.

[34] Fan, J., Du, H., Zhao, Y., Wang, Q., Liu, Y., Li, D. and Feng, J., 2020. Recent progress on rational design of bimetallic Pd based catalysts and their advanced catalysis. ACS Catalysis, 10(22), 13560-13583.

[35] Huang, J., Jones, A., Waite, T.D., Chen, Y., Huang, X., Rosso, K.M., Kappler, A., Mansor, M., Tratnyek, P.G. and Zhang, H., 2021. Fe (II) redox chemistry in the environment. Chemical Reviews, 121(13), 8161-8233.

[36] Sun, W., Wang, S., Yu, Z. and Cao, X., 2023. Characteristics and application of iron-based materials in heterogeneous Fenton oxidation for wastewater treatment: a review. Environmental Science: Water Research & Technology, 9(5), 1266-1289.

[37] Padilla-Cruz, A.L., Garza-Cervantes, J.A., Vasto-Anzaldo, X.G., García-Rivas, G., León-Buitimea, A. and Morones-Ramírez, J.R., 2021. Synthesis and design of Ag–Fe bimetallic nanoparticles as antimicrobial synergistic combination therapies against clinically relevant pathogens. Scientific Reports, 11(1), 5351.

[38] Shen, L., Wang, C., Abbas, A., Yu, C., Zhang, S., Zhang, X. and Zhang, C., 2019. Switching carbon nanodots from single emission to dual emission by one-step electrochemical tailoring in alkaline alcohols: implications for sensing and bioimaging. ACS Applied Nano Materials, 2(5), 2776-2784.

[39] Tang, J., Shen, L., Zhao, K., Peng, J., Chen, Q., Yu, C., Li, Y., Abbas, A., Wang, S. and Liu, Z., 2024. An ultra-sensitively ammonia-responsive gas sensor based on Ag@ sulfur nanosheets. Applied Surface Science, 643, 158574.

[40] Abbas, A., Mansoor, S., Nawaz, M.H., Chaudhry, A.A., Ijaz, K., Riaz, S. and Hayat, A., 2023. Growth of diazonium-functionalized ZnO nanoflakes on flexible carbon cloth for electrochemical sensing of acetone in the liquid phase. RSC Advances, 13(17), 11537-11545.

[41] Yu, W., Sisi, L., Haiyan, Y. and Jie, L., 2020. Progress in the functional modification of graphene/graphene oxide: A review. RSC advances, 10(26), 15328-15345.

[42] Li, T., Yin, W., Gao, S., Sun, Y., Xu, P., Wu, S., Kong, H., Yang, G. and Wei, G., 2022. The combination of two-dimensional nanomaterials with metal oxide nanoparticles for gas sensors: a review. Nanomaterials, 12(6), 982.

[43] Hamza, A., Ho, K.C. and Chan, M.K., 2024. Recent development of substrates for immobilization of bimetallic nanoparticles for wastewater treatment: a review. Environmental Science and Pollution Research, 31(28), 40873-40902.

[44] Kabiri, B. and Heidari, H., 2025. Synthesis and catalytic activity of silver-reduced graphene oxide and silver-magnetite-reduced graphene oxide nanocomposites in the reduction of 4-nitrophenol. Scientific Reports, 15(1), 14539.

[45] Rando, G., Sfameni, S., Galletta, M., Drommi, D., Cappello, S. and Plutino, M.R., 2022. Functional Nanohybrids and Nanocomposites development for the removal of environmental pollutants and bioremediation. Molecules, 27(15), 4856.

[46] Abbas, A., Hussain, M.A., Sher, M., Abbas, N.S. and Ali, M., 2017. Modified hydroxyethylcellulose: a regenerable super-sorbent for $Cd^{2+}$ uptake from spiked high-hardness groundwater. Cellulose Chemistry and Technology, 51, 167-174.

[47] Hussain, M.A., Zaman, S., Abbas, A., Tahir, M.N., Amin, M., Hussain, S.Z. and Hussain, I., 2020. Sodium hyroxyethylcellulose adipate: An efficient and reusable sorbent for cadmium uptake from spiked high-hardness ground water. Arabian Journal of Chemistry, 13(1), 2766-2777.

[48] Kanwal, M., Sher, M., Abbas, A., Akhtar, S., Siddique, A.B., ul Hasan, M.N., Assad, N., Alhazmi, H.A. and Amin, H.M., 2025. Dual colorimetric sensing of Hg (II) and Fe (III) using sulfanilamide-stabilized silver nanoparticles and evaluating their photodegradation and antibacterial properties. Journal of Water Process Engineering, 75, 107981.

[49] Siddique, A.B., Shaheen, M.A., Abbas, A., Zaman, Y., Amin, H.M., Alam, M.M., Alharbi, N.K., Alshehri, F., Shami, A., Al-Joufi, F.A. and Ali, A., 2025. Sunlight-assisted greenly synthesised silver nanoparticles for highly selective mercury ion sensing, biomedical and photocatalytic applications. International Journal of Environmental Analytical Chemistry, 1-23.